ORIGINAL RESEARCH ARTICLE

Eutectic Composition Design, Microstructure, and Room Temperature Mechanical Property of NiAl-Cr-Ta Three-Phase Alloy

LEI WANG, LUHAN GAO, JUN SHEN, YUNPENG ZHANG, GANG LIU, PENGKANG ZHAO, and GUOJUN ZHANG

In this paper, NiAl-33Cr-4.5Ta (at. pct) near-eutectic alloy consisting of NiAl, α-Cr and Laves is successfully designed by JMatPro software and verified by experiments. TEM result reveals that it exists an orientation relationship between each two phases. Directionally solidified (DS) alloy has a well-aligned microstructure and possesses a fracture toughness (9.8 $MPa \cdot m^{1/2}$). Moreover, the DS alloy has a tensile ductility (1.4 pct) at room temperature. Fracture behavior is analyzed by the crack propagation and fracture surface.

LEI WANG, LUHAN GAO, YUNPENG ZHANG, GANG LIU, and GUOJUN ZHANG are with the School of Materials Science and Engineering, Xi'an University of Technology, Xi'an, 710048, P.R. China. Contact e-mail: wang_lei@xaut.edu.cn; shenjun@nwpu.edu.cn; zhangguojun@xaut.edu.cn JUN SHEN is with the State Key Laboratory of Solidification Processing, Northwestern Polytechnical University, Xi'an, 710072, P.R. China. PENGKANG ZHAO is with the School of Mechanical and Instrument Engineering, Xi'an University of Technology, Xi'an, 710048, P.R. China.

Manuscript submitted August 25, 2021; accepted January 23, 2022.
Article published online February 10, 2022

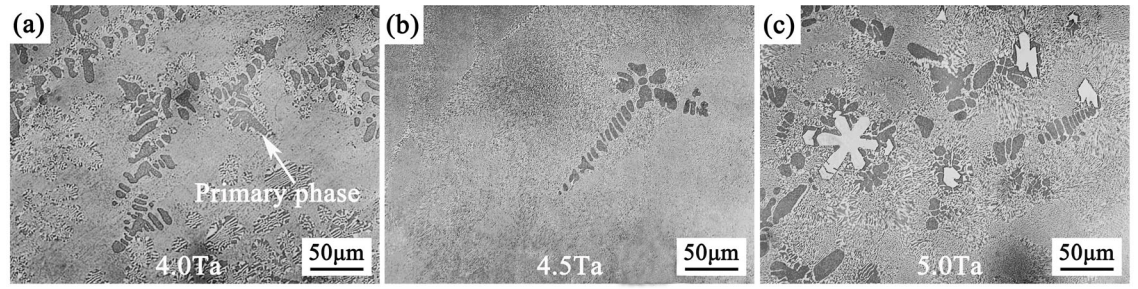

Design of NiAl-33Cr-4.5Ta (at.%) near eutectic alloy (arc melting)

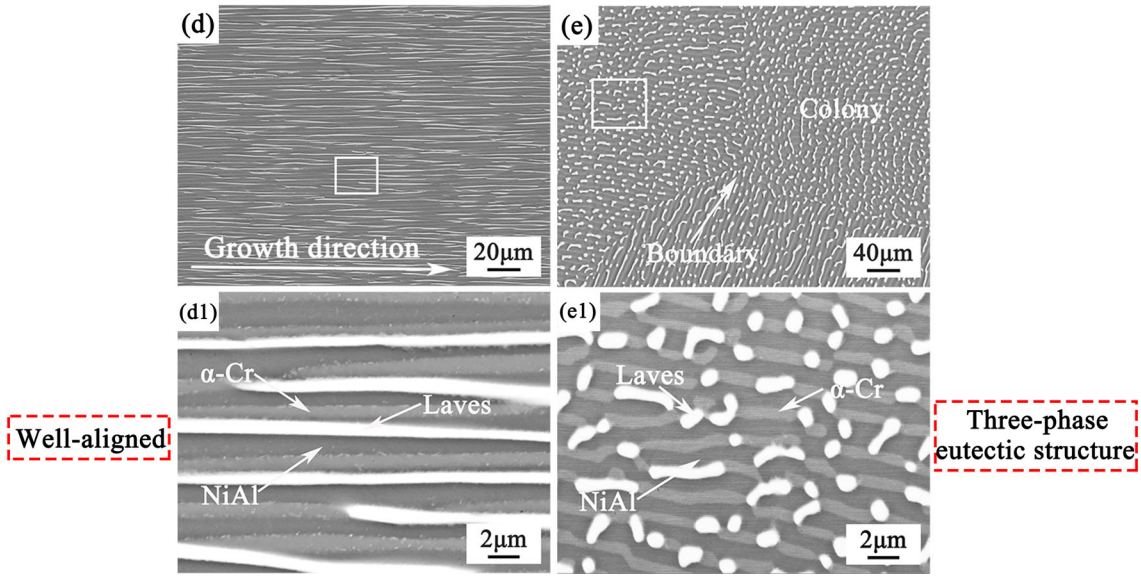

Longitudinal (d,d1) and transverse (e,e1) microstructures of DS NiAl-33Cr-4.5Ta alloy at 6 μm/s

https://doi.org/10.1007/s11661-022-06611-7

ATTRACTIVE combinations of high melting point, low density, excellent oxidation resistance, and high thermal conductivity make NiAl a potential candidate for replacing superalloys in aircraft engine.[1,2] However, its practical application is limited because of low room temperature fracture toughness (4 to 6 MPa·m$^{1/2}$) and poor elevated-temperature strength (~ 50 MPa at 1027 °C).[3] Alloying (Cr, Mo, V, Ta, Nb, W) NiAl to form NiAl-based eutectic alloys is a common way to improve the property, like two-phase eutectic alloys: NiAl-Cr (~ 20.38MPa·m$^{1/2}$),[4,5] NiAl-Mo (~ 19.36MPa·m$^{1/2}$),[6–11] NiAl-Cr(Mo) (~ 21.6 MPa·m$^{1/2}$),[4,12–19] NiAl-V (28.6 to 32.0MPa·m$^{1/2}$),[20–22] NiAl-Ta (5.1MPa·m$^{1/2}$),[23] NiAl-Nb (4.0 MPa·m$^{1/2}$)[23,24], and NiAl-W.[25] Among these alloys, the former four alloys possess higher fracture toughness compared to NiAl-Ta and NiAl-Nb eutectic alloys; however, NiAl-Ta and NiAl-Nb eutectic alloys possesses higher elevated-temperature creep strength. According to the previous comparison results,[4] NiAl-Cr(Mo) eutectic alloy possesses the better combining properties. However, it still does not meet the requirement of application.

In order to further improve the properties, many investigations are conducted in NiAl-Cr(Mo) eutectic alloy, like alloying Hf or rare earth elements.[26–32] The elevated-temperature strength can be improved; however, the fracture toughness significantly decreases (about 6.24 MPa·m$^{1/2}$ for NiAl-Cr(Mo)-Hf[28]). Then, some investigations in our group are conducted to improve the above-mentioned properties. Firstly, the investigation object is adjusted for NiAl-36Cr-6Mo hypereutectic alloy. The fracture toughness is enhanced to 26.15 MPa·m$^{1/2}$ by increasing the volume fraction of Cr(Mo) strengthening-toughness phase.[33] The elevated-temperature tensile strength is also improved (513 MPa at 1000 °C[34]) compared to NiAl-28Cr-6Mo eutectic alloy (374 MPa at 1000 °C[34] or 348 MPa at 1093 °C[35]). Secondly, alloying (like Hf, Dy, and Fe) based on NiAl-Cr(Mo) hypereutectic alloy is conducted.[36–41] It is worth mentioning that the NiAl-Cr(-Mo)-(Hf,Dy)-4Fe alloy possesses high fracture toughness (18.4 MPa·m$^{1/2}$[36]) compared to the previous Hf-containing NiAl-Cr(Mo) eutectic alloy (about 6.24 MPa·m$^{1/2}$[28]). Thirdly, the microstructural stability of

NiAl-Cr(Mo) eutectic alloy at high temperatures (900-1100 °C) is investigated.[17,18] Moreover, the design of NiAl-based eutectic alloys are conducted to improve the mechanical properties.[42,43] However, up to now, it is difficult to achieve the balance of fracture toughness and strength for NiAl-based two-phase eutectic alloys.

Previous studies reported that α-Cr(Mo), α-Cr, α-Mo, or α-V can improve the fracture toughness,[4–22] and Laves phase (NiAl-Ta and NiAl-Nb) can efficiently enhance the high temperature strength.[23,24] Thus, it may be a good way that adding several proper elements is to form a three-phase eutectic composite which is composed of NiAl, α phase, and Laves phase. Three-phase eutectic composite will possess the good fracture toughness and high temperature strength. It is well known that Cr is an element of excellent oxidation resistance, and Ta is a typical refractory element. Also, the above discussion implies that the addition of Cr and Ta to NiAl may result in the formation of α-Cr and Laves phase. Therefore, in this paper, we try to design the eutectic composition of NiAl-Cr-Ta three-phase alloys by adjusting Cr and Ta content. In addition, previous studies reported that directional solidification (DS) is an excellent way to improve the mechanical property of NiAl-based eutectic alloy compared to the conventional casting.[4,6,14,44,45] Generally, in the directional solidification process, no grain boundary or a small amount of grain boundaries occur, and the unidirectional well-aligned microstructures can be obtained, thus improving the mechanical properties. Thus, we will primarily investigate the microstructure and room temperature mechanical property of DS NiAl-Cr-Ta three-phase eutectic alloy in this paper. It needs to be mentioned that, compared to our previous studies (two-phase eutectic mentioned in the second paragraph), the biggest difference is the design of novel NiAl-Cr-Ta three-phase eutectic alloy in this paper.

The eutectic composition was primarily predicted by calculating solidification paths of alloys using JMatPro7.0 software (Ni-based database) and then verified by experiments (arc melting). Correspondingly, the near-eutectic composition (NiAl-33Cr-4.5Ta, at. pct) is determined. The ingots of NiAl-33Cr-4.5Ta near-eutectic alloy were prepared using a vacuum induction melting. The rods with 7mm in diameter, cut from the ingots by electro-discharge machining (EDM), were directionally solidified at the withdrawal rate of 6 μm/s. The furnace temperature was kept at 1660 ± 10 °C. The description of microstructural observation is similar to our previous study.[43] Three-point bending specimens with the nominal dimensions of 3 mm×6 mm×28 mm were performed in an Instron 3382 universal test machine with a cross-head speed of 0.05 mm/min. Tensile tests were performed at room temperature and a cross-head speed of 0.025 mm/min (3×10^{-5} s^{-1}) in an Instron 3382 universal test machine. The tensile specimen has a gauge length of 13.8 mm. The tensile direction is parallel to the growth direction.

Figure 1(a) gives the solidification path and phase composition of NiAl-33Cr-4Ta (at. pct) alloy using JMatPro software. It can be seen that two phases can simultaneously forms at 1450 °C. Although the constituent phases are only two phases in the calculation results which are different from the experiment results (three-phase eutectic), it does not hinder us to deduce that NiAl-33Cr-4Ta (at. pct) may be a near-eutectic composition. However, from the experimental results, a number of primary dendrite (9.9 pct) is still observed in the NiAl-33Cr-4Ta alloy, as shown in Figure 1(b). Although some differences exist, it is deduced that NiAl-33Cr-4Ta (at. pct) may be deviated from the eutectic composition to a small degree. Then, the close composition alloys [like NiAl-33Cr-xTa (x = 4.5, 5 at. pct)] are prepared, as illustrated in Figures 1(c) and (d). It is found that the volume fraction of primary dendrite is low (~3.5 pct) in NiAl-33Cr-4.5Ta alloy. Thus, it is determined that NiAl-33Cr-4.5Ta (at. pct) is a near-eutectic alloy. Also, it implies that it is a good strategy to design NiAl-Cr-Ta eutectic alloy (even NiAl-based eutectic alloys) by calculating solidification paths using JMatPro software.

Figure 2 shows the longitudinal and transverse microstructures of DS NiAl-33Cr-4.5Ta near-eutectic alloy. Firstly, it can be seen that the complete eutectic structures are obtained by directional solidification. Secondly, the longitudinal microstructure shows that the alternate three phases are unidirectional and well aligned, as displayed in Figures 2(a) and (b). From the transverse microstructure, it consists of eutectic colonies which are composed of black phase, lamellar gray phase, and rod-like/lath-like white phase (three-phase eutectic). The three phases are identified as NiAl, α-Cr, and Cr_2Ta [Laves phase, which is further identified by TEM (Figure 3)], respectively. The specific compositions of three phases are given in Table I.

Furthermore, to closely examine the three phases and determine the relationship between each two phases, we have conducted a TEM analysis. Figure 3(b) shows the complex select area electron-beam diffraction patterns (SAEDs) of NiAl and α-Cr phase, and it establishes a cube-on-cube orientation relationship between them, *i.e.*, $[\bar{1}11]_{NiAl}//[\bar{1}11]_{\alpha\text{-}Cr}$ and $(101)_{NiAl}$ // $(101)_{\alpha\text{-}Cr}$. This is similar to the orientation relationship between NiAl and Cr(Mo) phases in NiAl-Cr(Mo) eutectic alloy[26,27]. Figure 3(c), (d) shows the complex SAEDs of NiAl and Laves phase, α-Cr and Laves phase, respectively. It reveals a semi-coherent relationship of NiAl and Laves phase, *i.e.*, $[\bar{1}11]_{NiAl}$ // $[\bar{1}2\bar{1}6]_{Laves}$ and $(\bar{1}\bar{1}0)_{NiAl}$ // $(2\bar{2}01)_{Laves}$, and also reveals a semi-coherent relationship of α-Cr and Laves phase, *i.e.*, $[\bar{1}11]_{\alpha\text{-}Cr}$ // $[\bar{1}2\bar{1}6]_{Laves}$ and $(\bar{1}\bar{1}0)_{\alpha\text{-}Cr}$ // $(2\bar{2}01)_{Laves}$. The lattice mismatch parameter is 2.8 pct, and the small parameter favors the stability of microstructure at high temperature.[28] In addition, we also determine the crystal structure of Laves with hcp, as shown in Figure 3(e), (f).

Subsequently, the room temperature fracture toughness of DS NiAl-33Cr-4.5Ta near-eutectic alloy is evaluated. The DS alloy possesses a fracture toughness (9.8 $MPa{\cdot}m^{1/2}$) which is significantly higher than that of as-cast NiAl alloy (4-6 $MPa{\cdot}m^{1/2}$[3,46]). Furthermore, the deflection of side surface crack of DS alloy implies that the crack propagation suffers from some resistances, as displayed in Figure 4(a). The α-Cr phase and the

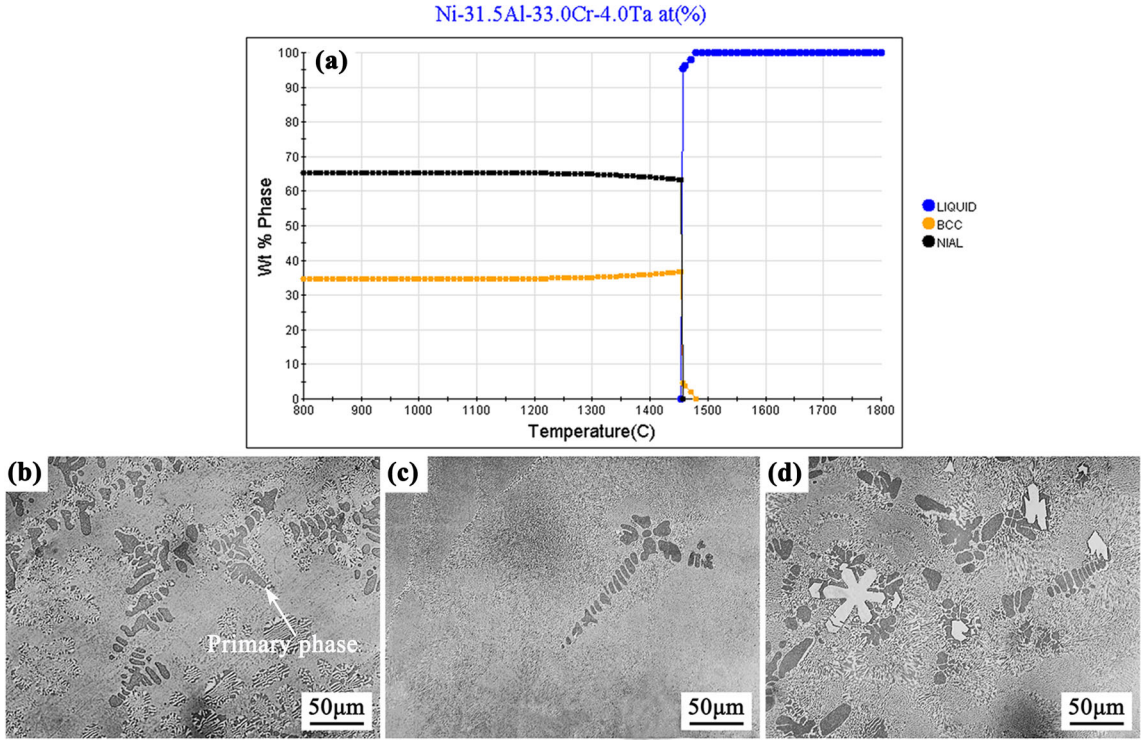

Fig. 1—(*a*) Solidification path and phase composition of NiAl-33Cr-4Ta (at. pct) alloy by JMatPro, and microstructures of NiAl-Cr-Ta alloys with different compositions prepared by arc melting: (*b*) NiAl-33Cr-4Ta, (*c*) NiAl-33Cr-4.5Ta, and (*d*) NiAl-33Cr-5Ta (at. pct).

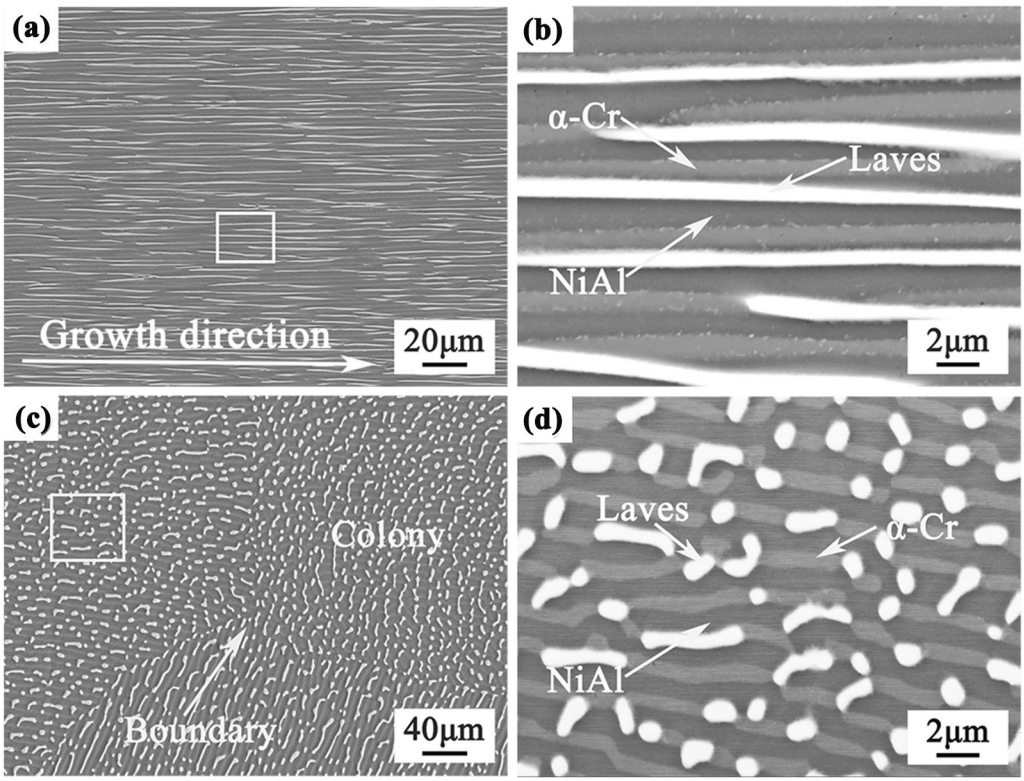

Fig. 2—BSE images of longitudinal (*a* and *b*) and transverse (*c* and *d*) microstructures of DS NiAl-33Cr-4.5Ta near-eutectic alloy.

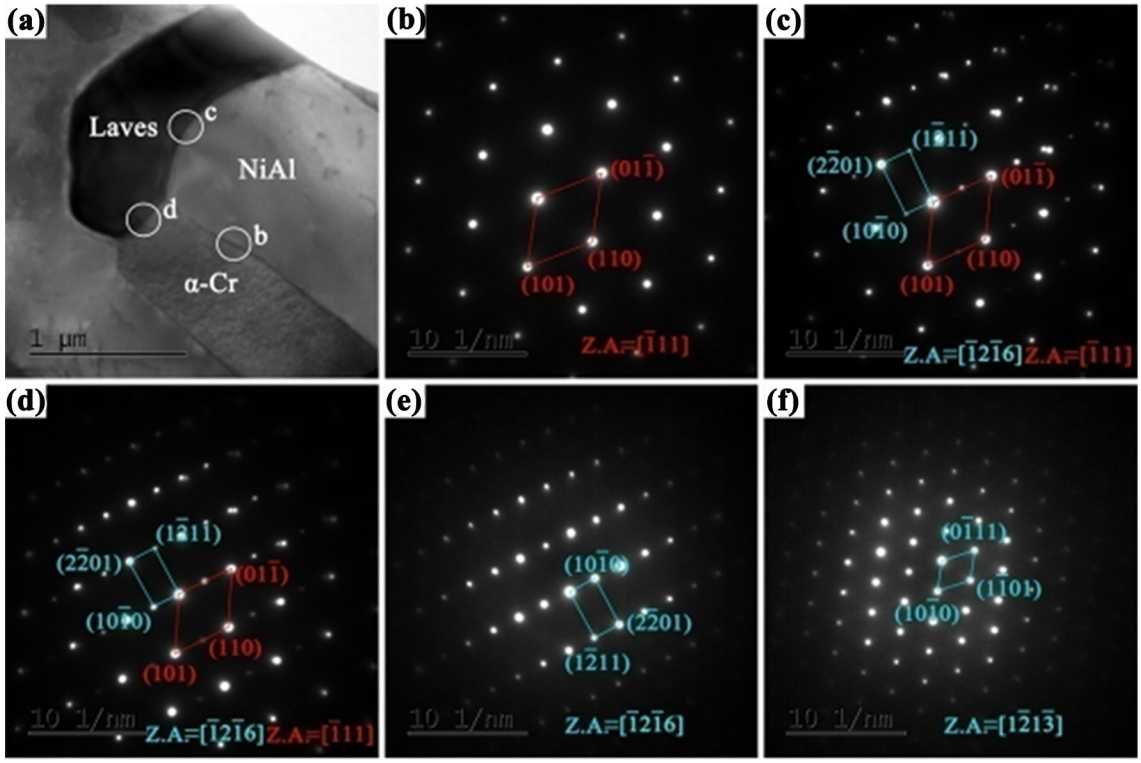

Fig. 3—(*a*) Bright-field TEM images of NiAl, α-Cr and Laves phases, (*b*) complex SAEDs of NiAl and α-Cr phase, (*c*) complex SAEDs of NiAl and Laves phase, (*d*) complex SAEDs of α-Cr and Laves phase, and (*e*, *f*) SAEDs of Laves phase.

Table I. Compositions of Constituent Phases of DS NiAl-33Cr-4.5Ta Near-Eutectic Alloy

Phase	Ni (At. Pct)	Al (At. Pct)	Cr (At. Pct)	Ta (At. Pct)
Black	45.86±0.39	44.80±0.29	8.58±0.13	0.71±0.07
Gray	5.30±0.29	10.26±0.30	82.75±0.15	1.6±0.18
White	10.31±0.15	6.20±0.20	52.55±0.67	31.06±0.44

interface between each two phases have some resistances to crack propagation, like crack bridging and interface debonding, as displayed in Figure 4(b). It reveals that the introduction of α-Cr and Lave phases can bring a certain contribution to the fracture toughness. However, the fracture toughness of present alloy is lower than that of DS NiAl-Cr(Mo) eutectic alloy (21.6 $MPa{\cdot}m^{1/2}$[4]). This should be attributed to the intrinsic brittleness of Laves phase in present alloy. The planar fracture surface and the cleavage of NiAl phase demonstrate the brittle characteristic. In addition, to our best knowledge, aerospace applications generally require the fracture toughness of at least 15 $MPa{\cdot}m^{1/2}$[47] or 20 $MPa{\cdot}m^{1/2}$.[48] Therefore, the fracture toughness (9.8 $MPa{\cdot}m^{1/2}$) of present alloy is still unable to meet the requirements of aerospace applications. The fracture toughness of present alloy needs to be further improved in future.

Correspondingly, the room temperature tensile property of the DS NiAl-33Cr-4.5Ta near-eutectic alloy is evaluated. Figure 5(a) gives the tensile engineering stress–strain curve of the alloy. The result shows that the alloy broke without prior yielding. The tensile strength is 254 MPa, and the ductility is 1.4 pct. The tensile strength of the alloy is higher than that of NiAl (229 MPa[49]) and close to that of NiAl-Cr(Mo)-Hf (255MPa[46]) and is lower than that of NiAl-Cr(Mo) (680MPa[35]). Its ductility is close to that of NiAl, NiAl-Cr(Mo), NiAl-Cr(Mo)-Hf, and NiAl-Mo (≤2.2 pct[35,44,46,49]). That is, NiAl and NiAl-based eutectic alloys possess poor ductility. Figures 5(b) through (f) shows the fracture characteristics of NiAl-Cr-Ta near-eutectic alloy. The whole fracture surface is almost planar [similar to the above fracture surface of toughness specimen (see Figure 4), and no necking and dimples occur during the fracture process, as shown in Figures 5(b) through (e). It implies that the alloy breaks in a brittle manner. From the magnified image [Figure 5(c)], the river-like cleavage pattern further reveals the brittle fracture characteristic. Moreover, the highly magnified image reveals the fracture characteristic of the constituent phases, as shown in Figure 5(f). In particular, the NiAl phase also shows a

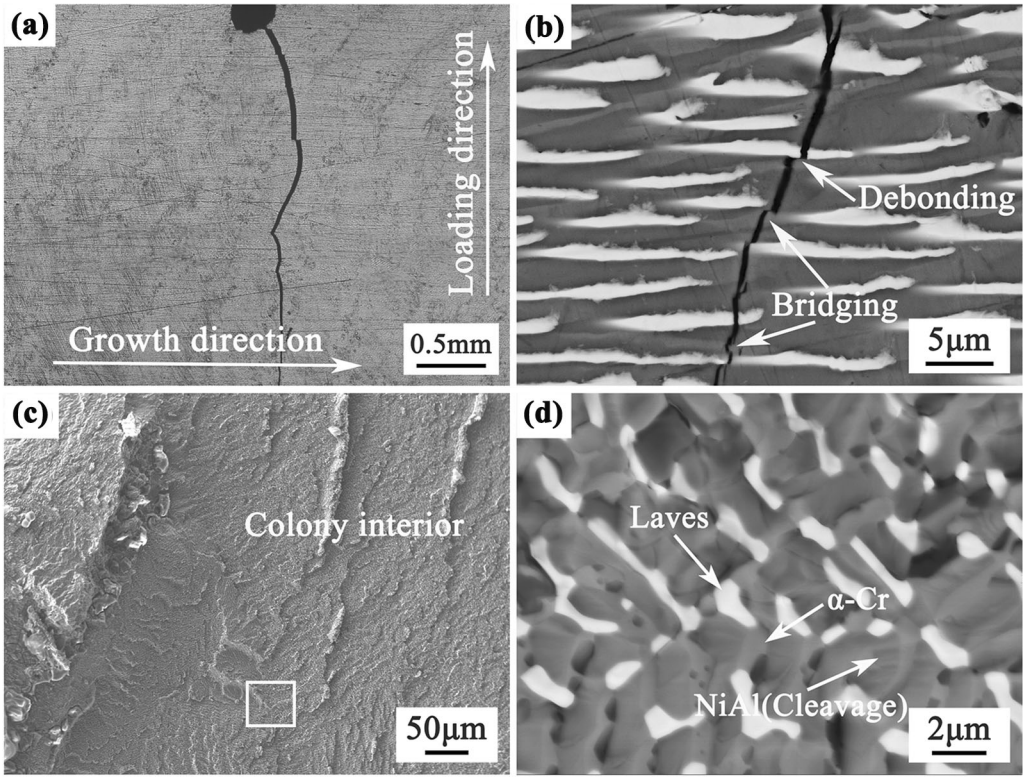

Fig. 4—(*a*, *c*) Lowly and (*b*, *d*) highly magnified images of crack propagation in the side surface and fracture surfaces of DS alloy after the three-point bending tests.

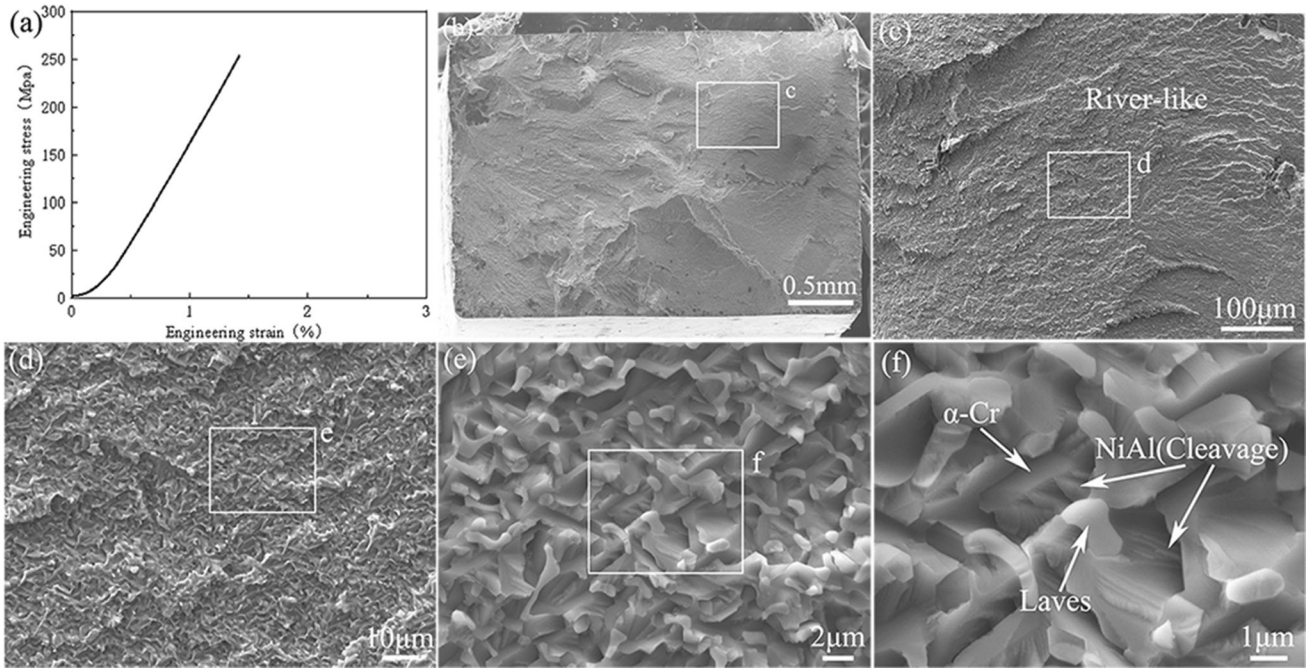

Fig. 5—(*a*) Tensile engineering stress–strain curve of DS NiAl-Cr-Ta near-eutectic alloy (6 μm/s) at room temperature, (*b*) the whole fracture surface image, and (*c*, *d*, *e*, and *f*) the magnified images of the closed rectangle area in (b, c, d, and e), respectively.

cleavage fracture characteristic, which is similar to that of toughness specimen (see Figure 4). The fracture characteristic also demonstrates its poor ductility.

In summary, it is a good strategy to design NiAl-Cr-Ta eutectic alloy (even NiAl-based eutectic alloy) by calculating solidification paths using JMatPro software. Directionally solidified NiAl-33Cr-4.5Ta (at. pct) three-phase near-eutectic alloy exhibits the well-aligned microstructure, and possesses a fracture toughness (9.8 $MPa{\cdot}m^{1/2}$) which is higher than that of NiAl (4-6 $MPa{\cdot}m^{1/2}$). The DS alloy possesses low room temperature tensile strength (254 MPa) which is slightly higher than NiAl (229 MPa) and close to that of NiAl-Cr(Mo)-Hf (255 MPa) and is lower than that of NiAl-Cr(Mo) eutectic alloy (680 MPa). Moreover, the DS alloy has a ductility (1.4 pct) which is similar to NiAl, NiAl-Cr(Mo), and NiAl-Mo eutectic alloy (≤2.2 pct).

ACKNOWLEDGMENTS

The authors appreciate the support of the National Natural Science Foundation of China (51501147, 52074219), Natural Science Basic Research Plan in Shaanxi Province of China (2019JM-438, 2021JM-338), and the fund of the State Key Laboratory of Solidification Processing in NPU (SKLSP202007).

CONFLICT OF INTEREST

The authors declare that they have no known competing financial interests or personal relationships that could have appeared to influence the work reported in this paper.

REFERENCES

1. K. Bochenek and M. Basista: *Prog. Aerospace Sci.*, 2015, vol. 79, pp. 136–46.
2. R. Darolia: *Intermetallics*, 2000, vol. 8, pp. 1321–27.
3. R.D. Noebe, R.R. Bowman, and M.V. Nathal: *Int. Mater. Rev.*, 1993, vol. 38, pp. 193–232.
4. D.R. Johnson, X.F. Chen, B.F. Oliver, R.D. Noebe, and J.D. Whittenberger: *Intermetallics.*, 1995, vol. 3, pp. 99–113.
5. G. Frommeyer, R. Rablbauer, and H.J. Schäfer: *Intermetallics*, 2010, vol. 18, pp. 299–305.
6. A. Misra, Z.L. Wu, M.T. Kush, and R. Gibala: *Mater. Sci. Eng. A*, 1997, vol. 239–240, pp. 75–87.
7. A. Gali, H. Bei, and E.P. George: *Acta Mater.*, 2010, vol. 58, pp. 421–28.
8. J.F. Zhang, J. Shen, Z. Shang, L. Wang, and H.Z. Fu: *Mater Charact.*, 2015, vol. 99, pp. 160–65.
9. L. Hu, G. Zhang, W. Hu, G. Gottstein, S. Bogner, and A. Bührig-Polaczek: *Acta Mater.*, 2013, vol. 61, pp. 7155–65.
10. J.F. Zhang, J. Shen, Z. Shang, Z.R. Feng, L.S. Wang, and H.Z. Fu: *Intermetallics*, 2012, vol. 21, pp. 18–25.
11. J. Kwon, M.L. Bowers, M.C. Brandes, V. Mccreary, I.M. Robertson, P.S. Phani, H. Bei, Y.F. Gao, G.M. Pharr, E.P. George, and M.J. Mills: *Acta Mater.*, 2015, vol. 89, pp. 315–26.
12. X.F. Chen, D.R. Johnson, R.D. Noebe, and B.F. Oliver: *J. Mater. Res.*, 1995, vol. 10, pp. 1159–70.
13. J.D. Whittenberger, S.V. Raj, I.E. Locci, and J.A. Salem: *Metall. Mater. Trans. A*, 2002, vol. 33A, pp. 1385–97.
14. S.V. Raj, I.E. Locci, J.A. Salem, and R.J. Pawlik: *Metall. Mater. Trans. A*, 2002, vol. 33A, pp. 597–612.
15. D. Yu, K. An, X. Chen, and H. Bei: *J. Alloys Compd.*, 2016, vol. 656, pp. 481–90.
16. D. Yu, H. Bei, Y. Chen, E.P. George, and K. An: *Scr. Mater.*, 2014, vol. 84–85, pp. 59–62.
17. L. Wang, G.J. Zhang, J. Shen, Y.P. Zhang, H.X. Xu, Y.H. Ge, and H.Z. Fu: *J. Alloys Compd.*, 2018, vol. 732, pp. 124–28.
18. L. Wang, J. Shen, G.J. Zhang, Y.P. Zhang, L.L. Guo, Y.H. Ge, L.H. Gao, and H.Z. Fu: *Intermetallics*, 2018, vol. 94, pp. 83–91.
19. L.F. Wei and Z.L. Zhao: *Corros. Sci.*, 2018, vol. 138, pp. 142–45.
20. S. Milenkovic and R. Caram: *Metall. Mater. Trans. A*, 2015, vol. 46A, pp. 557–65.
21. S. Milenkovic, A.A. Coelho, and R. Caram: *J. Cryst. Growth.*, 2000, vol. 211, pp. 485–90.
22. S.M. Joslin, X.F. Chen, B.F. Oliver, and R.D. Noebe: *Mater. Sci. Eng. A*, 1995, vol. 196, pp. 9–18.
23. D.R. Johnson, X.F. Chen, B.F. Oliver, R.D. Noebe, and J.D. Whittenberger: *Intermetallics*, 1995, vol. 3, pp. 141–52.
24. J.D. Whlttenberger, R. Reviere, R.D. Noebe, and B.F. Oliver: *Scr. Mater.*, 1992, vol. 26, pp. 987–92.
25. J.J. Gao, Z.L. Zhao, L.F. Wei, K. Cui, S.Y. Wang, N. Li, J.Y. Guo, S. Chen, Z.R. Hu, and Y.L. Liu: *Metall. Mater. Trans. A*, 2018, vol. 48, pp. 3575–83.
26. J.T. Guo, C.Y. Cui, Y.X. Chen, D.X. Li, and H.Q. Ye: *Intermetallics*, 2001, vol. 9, pp. 287–97.
27. C.Y. Cui, J.T. Guo, Y.H. Qi, and H.Q. Ye: *Scripta Mater.*, 2001, vol. 44, pp. 2437–41.
28. C.Y. Cui, J.T. Guo, Y.H. Qi, and H.Q. Ye: *Intermetallics*, 2002, vol. 10, pp. 1001–09.
29. J.T. Guo, K.W. Huai, Q. Gao, W.L. Ren, and G.S. Li: *Intermetallics*, 2007, vol. 15, pp. 727–33.
30. L.Y. Sheng, J.T. Guo, and H.Q. Ye: *Mater. Des.*, 2009, vol. 30, pp. 964–69.
31. L.Y. Sheng, J.T. Guo, W.L. Ren, Z.X. Zhang, Z.M. Ren, and H.Q. Ye: *Intermetallics*, 2011, vol. 19, pp. 143–48.
32. L.Y. Sheng, J.T. Guo, L.Z. Zhou, and H.Q. Ye: *Mater. Sci. Eng. A*, 2009, vol. 500, pp. 238–43.
33. Z. Shang, J. Shen, L. Wang, Y.J. Du, Y.L. Xiong, and H.Z. Fu: *Intermetallics*, 2015, vol. 57, pp. 25–33.
34. Z. Shang, J. Shen, L. Wang, Y.J. Du, Y.L. Xiong, and H.Z. Fu: *Mater. Charact.*, 2015, vol. 109, pp. 152–59.
35. J.M. Yang, S.M. Jeng, K. Bain, and R.A. Amato: *Acta Mater.*, 1997, vol. 45, pp. 295–305.
36. L. Wang, J. Shen, Z. Shang, and H.Z. Fu: *Scr. Mater.*, 2014, vol. 89, pp. 1–4.
37. L. Wang, J. Shen, Z. Shang, J.F. Zhang, Y.J. Du, and H.Z. Fu: *Mater. Sci. Eng. A*, 2014, vol. 607, pp. 113–21.
38. L. Wang, J. Shen, Z. Shang, J.F. Zhang, J.H. Chen, and H.Z. Fu: *Intermetallics*, 2014, vol. 44, pp. 44–54.
39. L. Wang and J. Shen: *J. Alloys Compd.*, 2016, vol. 663, pp. 187–95.
40. L. Wang and J. Shen: *Mater. Sci. Eng. A*, 2016, vol. 654, pp. 177–83.
41. L. Wang, C.L. Yao, J. Shen, Y.P. Zhang, T. Wang, H.X. Xu, L.H. Gao, and G.J. Zhang: *Mater. Sci. Eng. A*, 2019, vol. 744, pp. 593–603.
42. L. Wang, J. Shen, Y.P. Zhang, L.L. Guo, H.X. Xu, and H.Z. Fu: *Intermetallics*, 2017, vol. 84, pp. 11–19.
43. L. Wang, C.L. Yao, J. Shen, Y.P. Zhang, G. Liu, X.Y. Wu, and G.J. Zhang: *Mater. Sci. Eng. A*, 2022, vol. 830, p. 142325.
44. H. Bei and E.P. George: *Acta Mater.*, 2005, vol. 53, pp. 69–77.
45. L. Wang, J. Shen, Y.P. Zhang, and H.Z. Fu: *Mater. Sci. Eng. A*, 2016, vol. 664, pp. 188–94.
46. J.T. Guo: *Ordered Intermetallic Compound NiAl Alloy*, Science Press, Beijing, 2003.
47. J.J. Petrovic and A.K. Vasudevan: *Mater. Sci. Eng. A*, 1999, vol. 261, pp. 1–5.
48. D.M. Dimiduk: *Mater. Sci. Eng. A*, 1999, vol. 263, pp. 281–88.
49. C.T. Liu and J.A. Horton: *Mater Sci. Eng. A*, 1995, vol. 192(193), pp. 170–78.